A

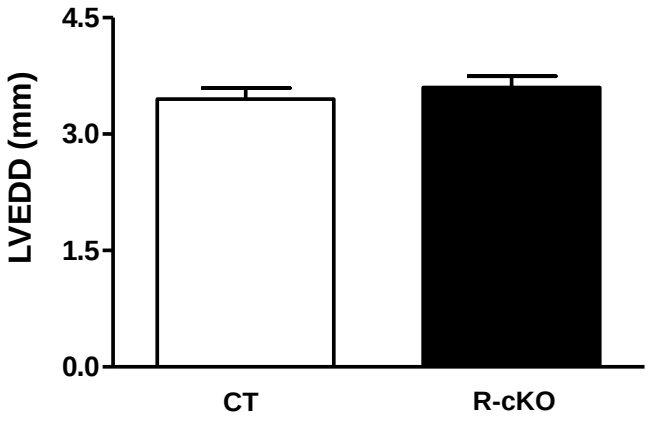

B

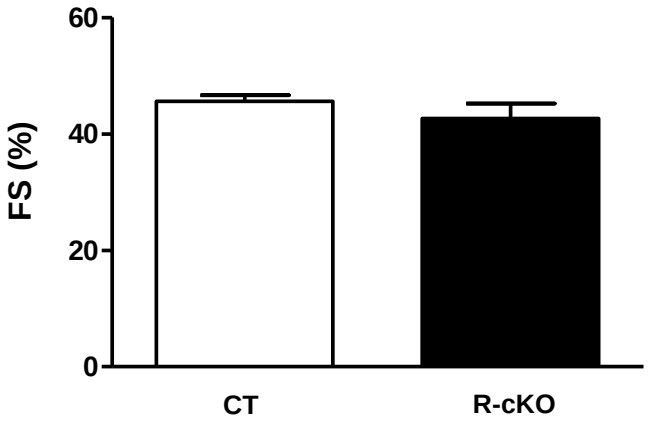

Figure S1. Baseline echocardiographic analysis in control and Rictor c-KO mice at two months of age, related to Figure 1.

Two-month old CT and R-cKO mice underwent echocardiographic analysis. Left ventricular end-diastolic diameter (A, LVEDD) and fractional shortening (B, FS) were measured. N=4. All data are expressed as mean ± SEM.

Figure S2

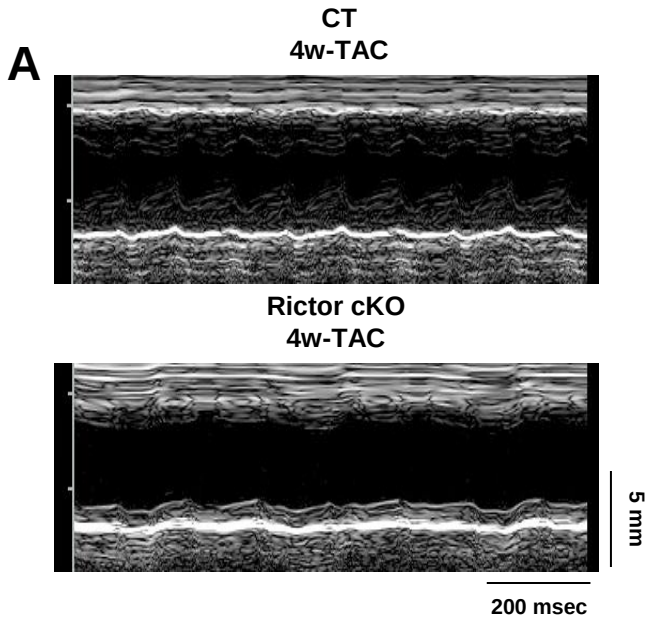
A
CT
4w-TAC
Rictor cKO
4w-TAC
5 mm
200 msec

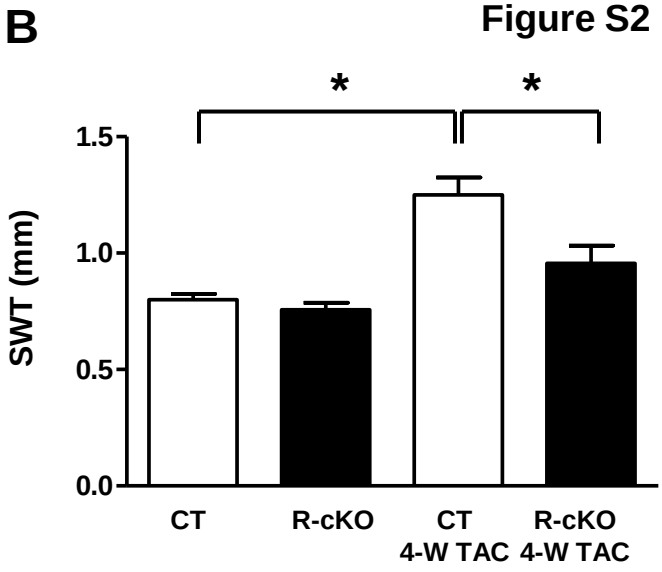
B
SWT (mm)
1.5
1.0
0.5
0.0
*
*
CT
R-cKO
CT
4-W TAC
R-cKO
4-W TAC

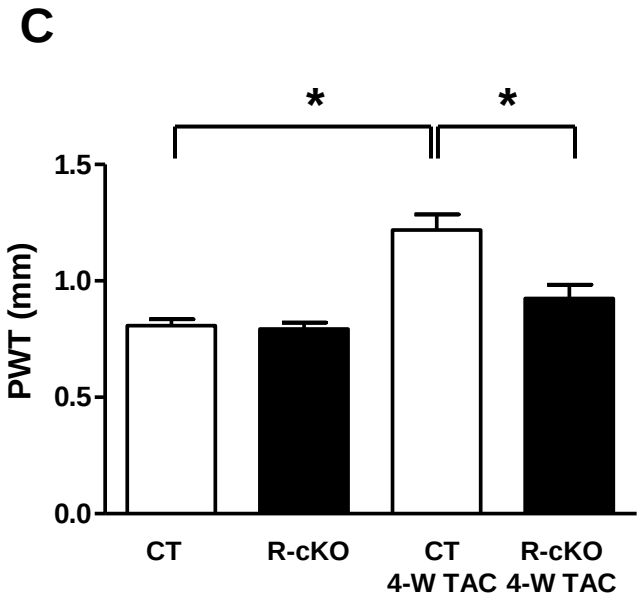
C
PWT (mm)
1.5
1.0
0.5
0.0
*
*
CT
R-cKO
CT
4-W TAC
R-cKO
4-W TAC

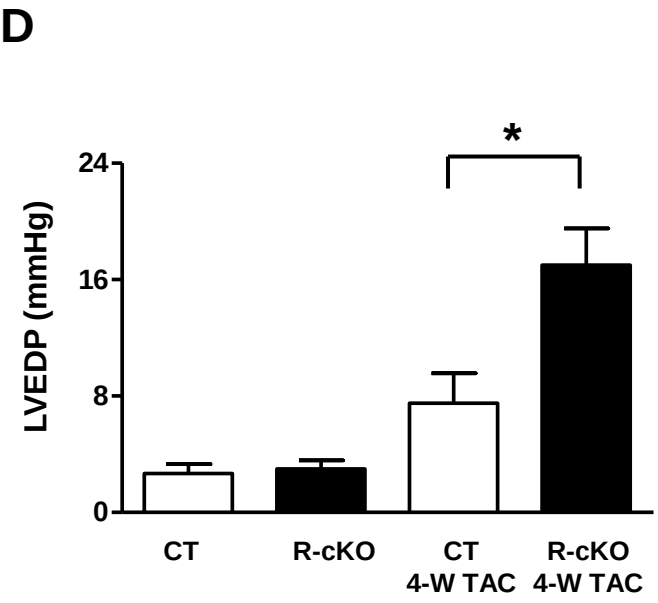
D
LVEDP (mmHg)
24
16
8
0
*
CT
R-cKO
CT
4-W TAC
R-cKO
4-W TAC

Figure S2. Echocardiographic and hemodynamic analyses in control and Rictor c-KO mice after transverse aortic constriction, related to Figure 2.

A-C. CT and R-cKO mice underwent echocardiographic analysis. Representative pictures are shown (A). Septum (SWT) and posterior wall thickness (PWT) were measured. N=7-8. **D.** CT and R-cKO mice underwent hemodynamic analysis. Left ventricular end-diastolic pressure were measured. All data are expressed as mean ± SEM. * $p<0.05$.

Figure S3

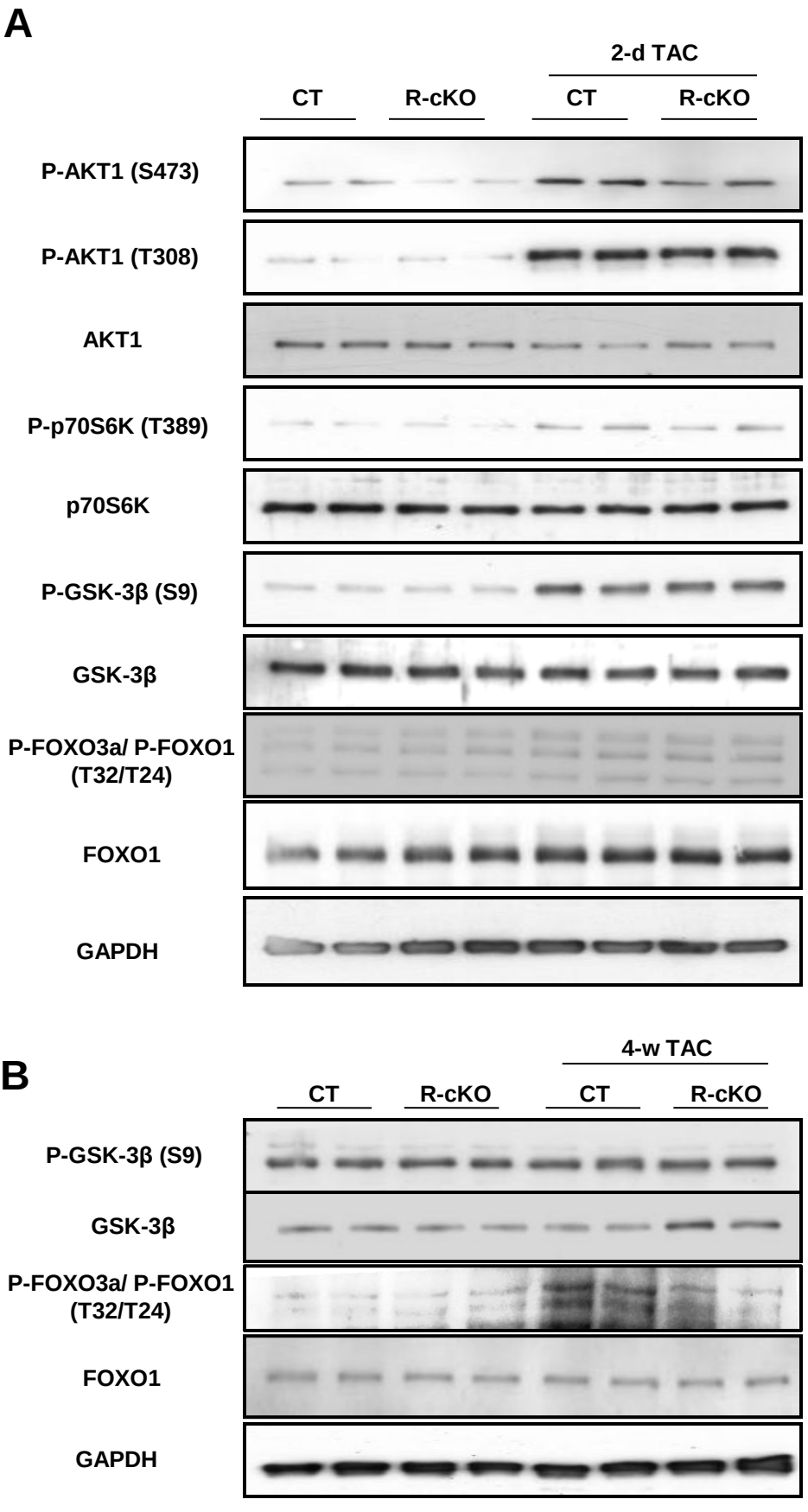
A
2-d TAC
CT
R-cKO
CT
R-cKO
P-AKT1 (S473)
P-AKT1 (T308)
AKT1
P-p70S6K (T389)
p70S6K
P-GSK-3β (S9)
GSK-3β
P-FOXO3a/ P-FOXO1 (T32/T24)
FOXO1
GAPDH
B
4-w TAC
CT
R-cKO
CT
R-cKO
P-GSK-3β (S9)
GSK-3β
P-FOXO3a/ P-FOXO1 (T32/T24)
FOXO1
GAPDH

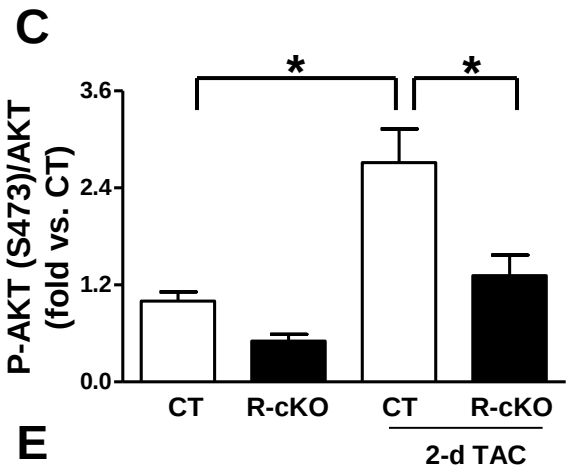
C
P-AKT (S473)/AKT
(fold vs. CT)
3.6
2.4
1.2
0.0
*
*
CT
R-cKO
CT
R-cKO
2-d TAC

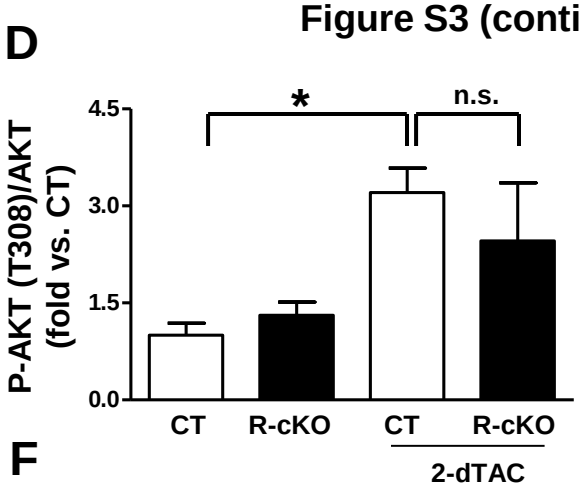
D
P-AKT (T308)/AKT
(fold vs. CT)
4.5
3.0
1.5
0.0
*
n.s.
CT
R-cKO
CT
R-cKO
2-dTAC

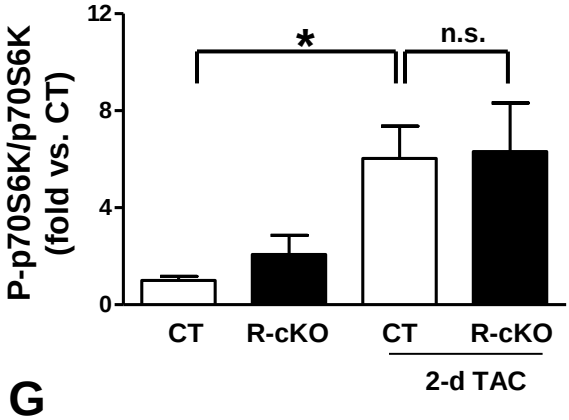
E
P-p70S6K/p70S6K
(fold vs. CT)
12
8
4
0
*
n.s.
CT
R-cKO
CT
R-cKO
2-d TAC

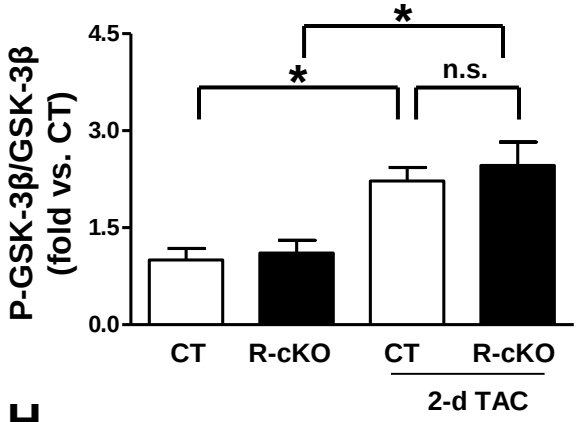
F
P-GSK-3β/GSK-3β
(fold vs. CT)
4.5
3.0
1.5
0.0
*
*
n.s.
CT
R-cKO
CT
R-cKO
2-d TAC

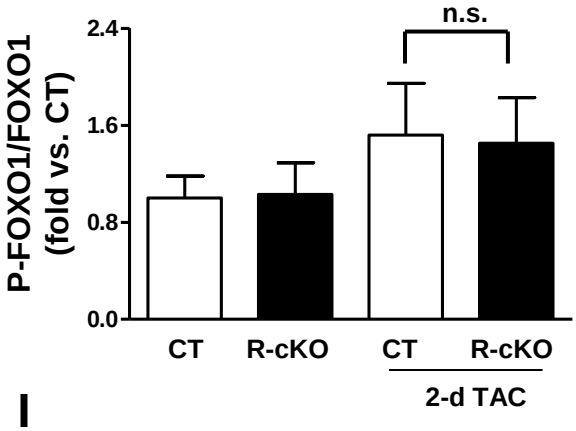
G
P-FOXO1/FOXO1
(fold vs. CT)
2.4
1.6
0.8
0.0
n.s.
CT
R-cKO
CT
R-cKO
2-d TAC

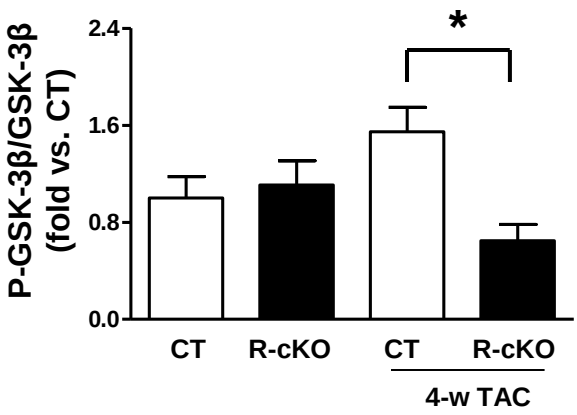
H
P-GSK-3β/GSK-3β
(fold vs. CT)
2.4
1.6
0.8
0.0
*
CT
R-cKO
CT
R-cKO
4-w TAC

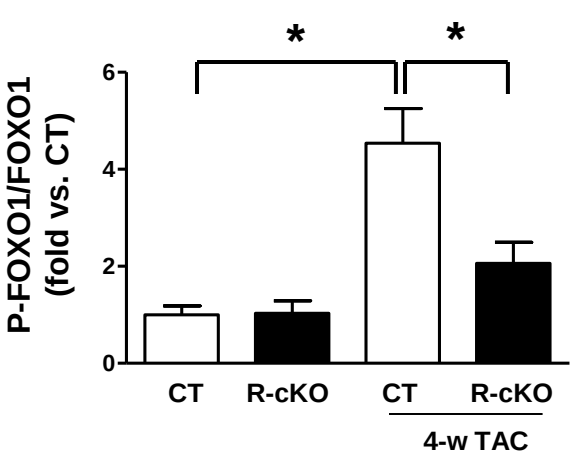
I
P-FOXO1/FOXO1
(fold vs. CT)
6
4
2
0
*
*
CT
R-cKO
CT
R-cKO
4-w TAC

Figure S3. Analysis of the conventional signaling pathways downstream of mTORC2 in the hearts of control and Rictor c-KO mice, related to Figure 4.

Levels of specified proteins were evaluated in the hearts of CT and R-cKO mice at baseline and after pressure overload. Representative immunoblots and densitometric analyses are shown. N=4-8. All data are expressed as mean ± SEM and as fold vs. CT. * $p<0.05$; n.s.= not significant.

Figure S4

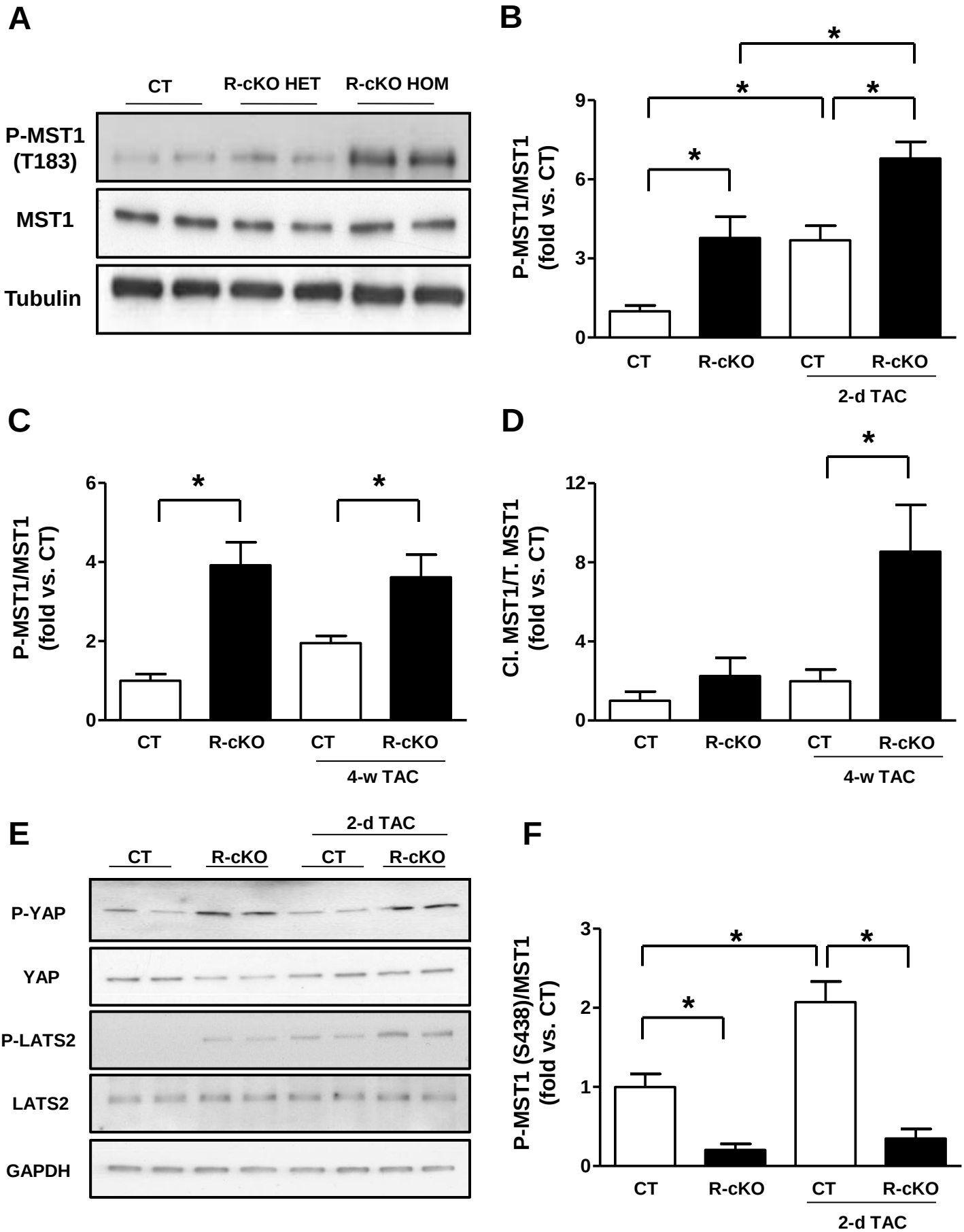
A
CT
R-cKO HET
R-cKO HOM
P-MST1 (T183)
MST1
Tubulin
B
P-MST1/MST1 (fold vs. CT)
CT
R-cKO
CT
R-cKO
2-d TAC
C
P-MST1/MST1 (fold vs. CT)
CT
R-cKO
CT
R-cKO
4-w TAC
D
Cl. MST1/T. MST1 (fold vs. CT)
CT
R-cKO
CT
R-cKO
4-w TAC
E
2-d TAC
CT
R-cKO
CT
R-cKO
P-YAP
YAP
P-LATS2
LATS2
GAPDH
F
P-MST1 (S438)/MST1 (fold vs. CT)
CT
R-cKO
CT
R-cKO
2-d TAC

Figure S4. Analysis of the Hippo pathway in the hearts of control and Rictor c-KO mice, related to Figure 4.

A. Immunoblot of cardiac phospho-MST1 (T183) and total MST1 levels in CT, heterozygous and homozygous R-cKO mice at baseline. **B-F.** CT and R-cKO mice were evaluated at baseline and after pressure overload. Cardiac levels of phosphorylated (T183), total and cleaved MST1 were evaluated by immunoblot analysis (B-D). Densitometric analyses are shown, whereas representative immunoblots are shown in Figure 4. N=4-6. Representative immunoblots of phospho-YAP (S127) and phospho-LATS2 (homologous to human T1041) together with immunoblots of the relevant total protein forms are shown (E). Cardiac levels of phosphorylated MST1 (S438) were also evaluated (F). Densitometric analyses are shown (F), whereas representative immunoblots are shown in Figure 5H. All data are expressed as mean ± SEM and as fold vs. CT. * $p<0.05$.

Figure S5

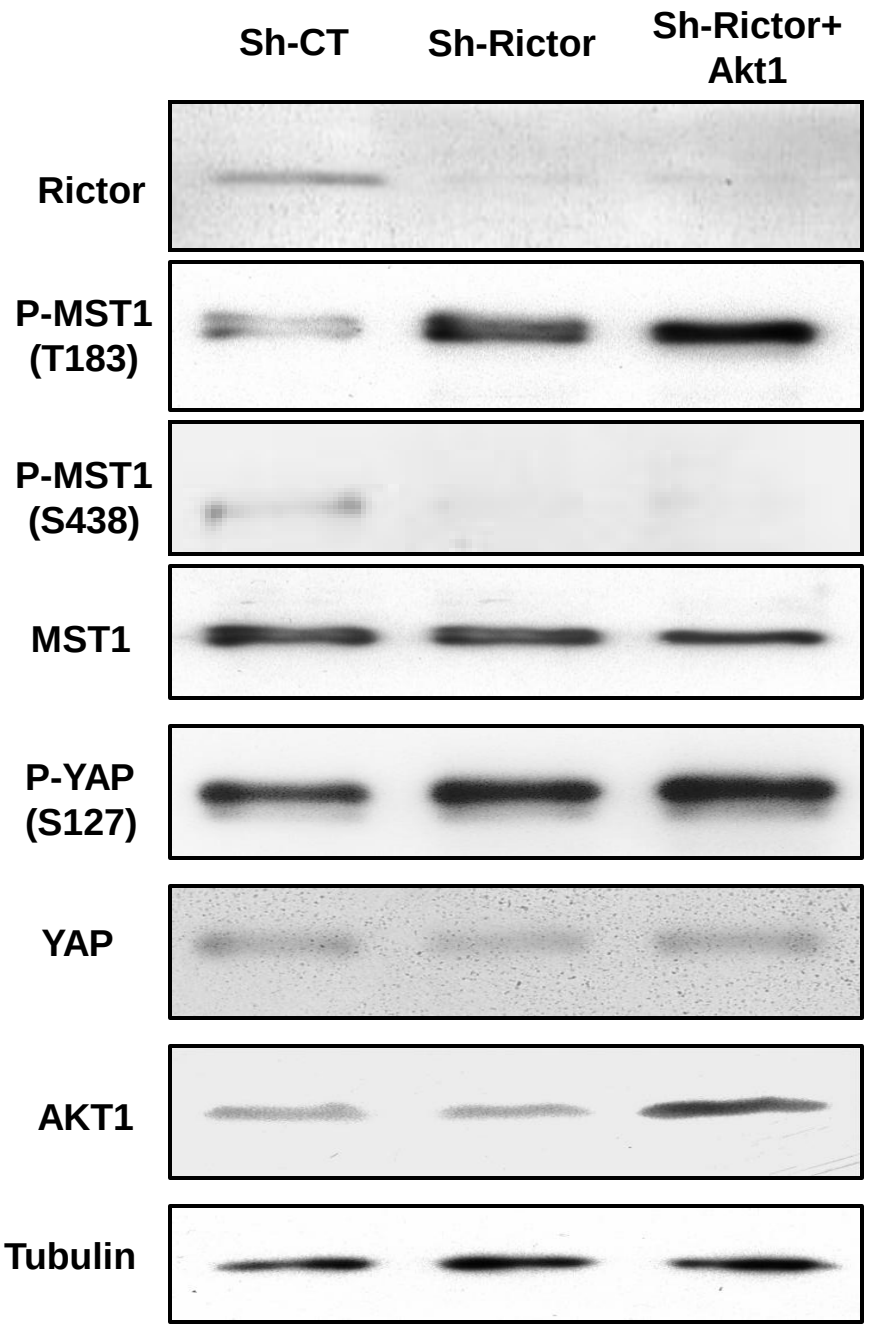
Sh-CT
Sh-Rictor
Sh-Rictor+ Akt1
Rictor
P-MST1 (T183)
P-MST1 (S438)
MST1
P-YAP (S127)
YAP
AKT1
Tubulin

Figure S5. mTORC2 regulates MST1 activity independently of AKT, related to Figure 5.

Cardiomyocytes were transduced with control adenovirus (Sh-CT) or with adenovirus expressing a short hairpin mRNA sequence targeting Rictor (Sh-Rictor) for 96 hours, with and without ad-LacZ or ad-CA-AKT for 48 hours. Levels of specified proteins were evaluated and representative immunoblots are shown.

Figure S6

A

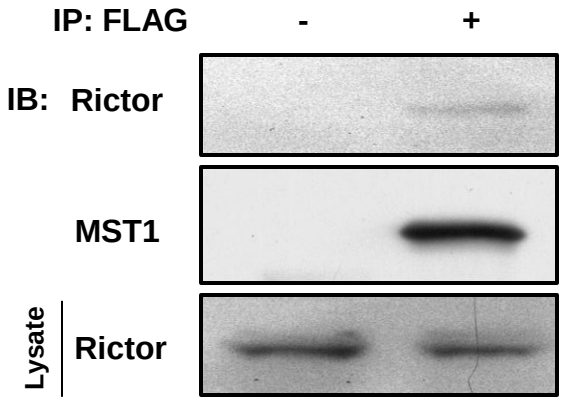

B

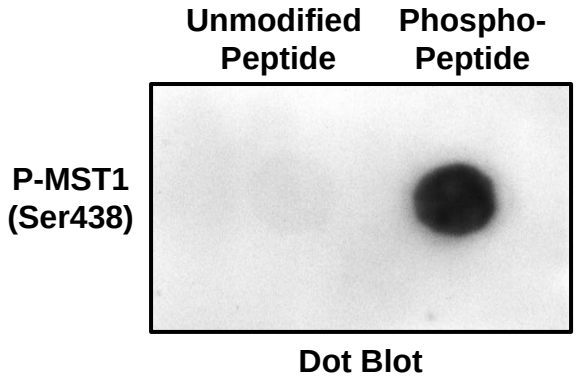

C

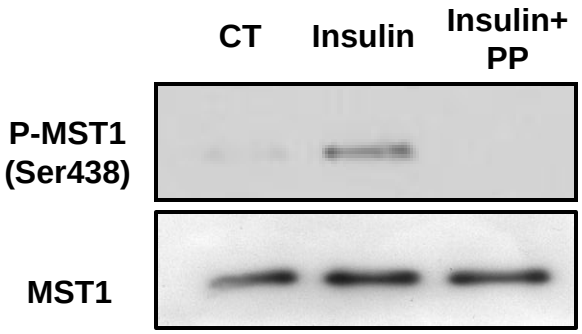

D

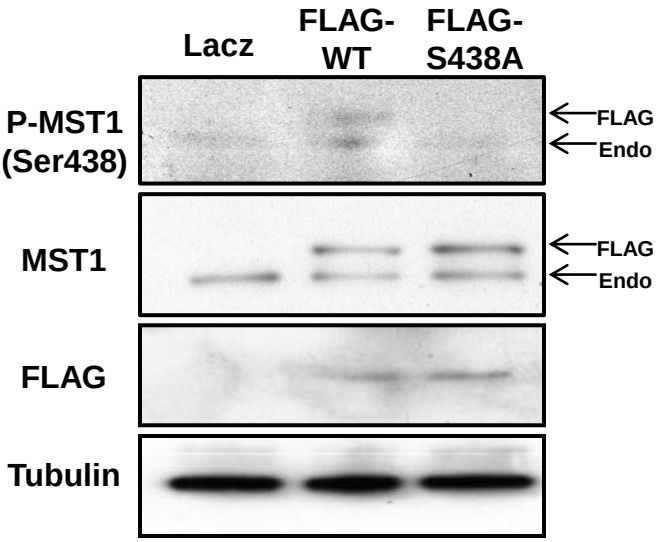

E

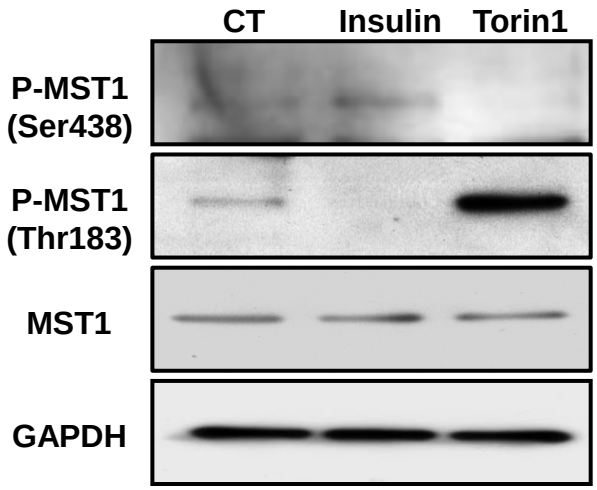

F

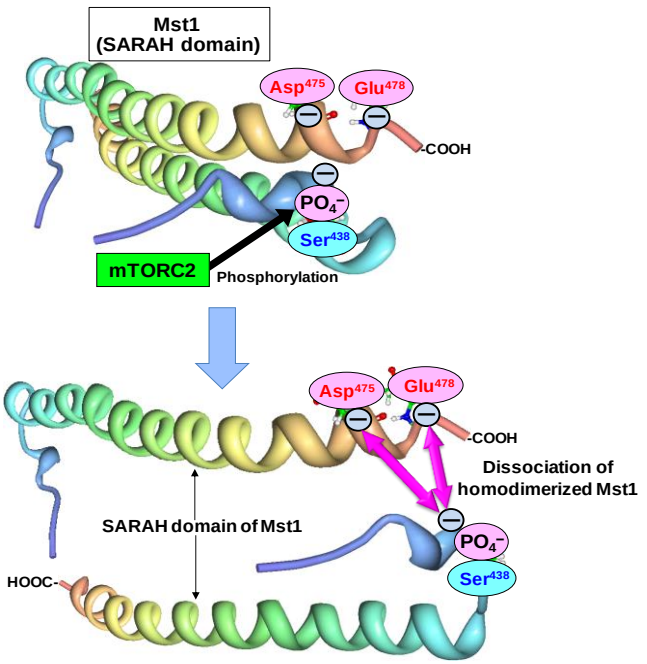

Figure S6. mTORC2 interacts with and phosphorylates MST1 at serine 438, related to Figures 5 and 6.

A. Cardiomyocytes were transduced with ad-FLAG-WT-MST1 for 48 hours. FLAG was immunoprecipitated and immunoblots of Rictor and MST1 are shown. **B.** Dot blot analysis using phospho-specific MST1 antibody (serine 438) tested against unmodified and phospho-peptide (10 ng). **C.** Cardiomyocytes were treated with insulin (200 nM) for 1 hour. Some protein lysates obtained from the insulin-treated cells were treated with protein phosphatase. Representative immunoblots of phosphorylated and total MST1 are shown. **D.** Cardiomyocytes were transduced with adenoviruses expressing the indicated proteins for 48 hours. Representative immunoblots of the indicated proteins are shown. Arrows specify endogenous (ENDO) and FLAG-tagged MST1. **E.** Cardiac fibroblasts were treated with insulin (200 nM) or Torin1 (100 nM) for 1 hour. Representative immunoblots of phosphorylated (S438 and T183) and total MST1 levels are shown. **F.** Crystallographic structure of SARAH domain dimer. The potential inhibitory effect of serine 438 phosphorylation on dimer formation is represented. RCSB PDB Protein Workshop 4.1.0 was used (PDB ID: 2JO8).